J. of Korean Oil Chemists' Soc.,
Vol. 16, No. 1, March 1999. 105~

접촉공정에서 건식각 특성

이창원* · 김재정* · 김대수, 이종대
충북대학교 화학공학과, *LG반도체 선행기술 개발 센터

The Dry Etching Characteristics in Contact Process

Chang Weon Lee* · Jae Jeong Kim*, Dae Su Kim and Jong Dae Lee

Dept. of Chem. Eng., Chungbuk National Univ., Cheongju, 360-763, Korea
**Advanced Tech. Development Center, LG Semicon Co., Ltd., Cheongju, Korea*

요 약 : P-type의 단결정 실리콘 위에 1000Å의 열산화막을 성장시킨후 5500Å의 다결정 실리콘으로 증착된 시료를 가지고 $HBr/Cl_2/He-O_2$ 혼합기체로 식각할 때 시료의 식각 특성에 관한 H_2-O_2 기체함량, RF 전력, 압력에 대한 영향을 XPS(X-ray photoelectron Spectroscopy)와 SEM(Scanning Electron Microscopy)으로 조사하였다. $HBr/Cl_2/He-O_2$ 혼합기체로 식각되는 동안 형성된 다결정 실리콘 식각속도는 H_2-O_2 함량 증가에 따라 증가하였으며 식각잔유물은 RF 전력과 압력변화에 의해 영향은 받지 않는 것으로 나타났으며, 다결정 실리콘 측벽에서의 증착속도는 낮은 RF전력과 높은 압력에서 높게 나타났다. 다결정 실리콘 식각 잔유물의 결합에너지는 안정한 SiO_2인 열산화막의 경우보다 높으므로 식각 잔유물은 $SiO_x(x>2)$의 화합결합을 가지는 산화물과 같은 잔유물로 생각된다.

I. INTRODUCTION

In dry etching process, the analysis of etch residue has been one of the main issues including etch rate, selectivity and etch profile to achieve high reliability of process and device performance. Etch residue has been studied by many researchers for various materials such as silicon, silicon dioxide, GaAs and so on. It has been recognized by many workers [1)~3)] that the addition of chemically active gases such as oxygen, hydrogen, or nitrogen to fluorocarbon plasma etching discharges usually results in often selective changes in the etch rates of silicon, silicon dioxide, and other materials of interest in semiconductor device manufacture. The addition of chemically active species also results in the effect of etch residue formation. When silicon and silicon dioxide are etched by fluorocarbon plasma, etch residue of (CF)x groups is generally formed on the etched surface[2),4)~10)]. Oehrlein et al.[8)] investigated fluorcarbon film deposition onto silicon and its influence on the measured silicon etch rate in CF_4/H_2 reactive ion etching as a function of CF_4/H_2 feed gas composition, total gas flow and applied RF power. They have observed at first a monotonic rise in deposited fluorocarbon film thickness with increasing RF power and at high RF power levels a dramatic decrease in the C,F-layer thickness.

Surface characterization was undertaken by many researchers[3)~13)] using x-ray photoelectron spectroscopy to determine the composition and chemical bonding in the near-

surface region of the etched samples. They reported that when material such as silicon, silicon dioxide was etched by fluorocarbon containing plasma, C,F-film could be explained by the presence of C-C and/or C-H, C-CF, CF, CF_2, and CF_3 type bonding. As mentioned, the physical and chemical processes underlying plasma etching are still only incompletely understood. Also, redeposition mechanism of etch product and active species is incompletely understood because of the complex phenomena in the plasma state although many researchers[9,11] try to examine redeposition mechanism.

Recently, more attention has been given to hydrogen bromide gas (HBr) for silicon, Ⅲ-Ⅴ, Al alloy, nitride and polysilicon RIE due to its highly selective silicon etch over silicon dioxide and for a lower loading effect chlorine based gases.[16~20] The extremely low reaction probability of the bromine atom on a silicon surface at thermal energy indicates that ion bombardment will play an important role in enhancing the surface reaction in the plasma and no sidewall passivation will be required to achieve anisotropic profile.[20] Tsou[20] also showed that HCl based plasma have a strong loading effect compared to HBr plasma and reported that HBr plasmas have a very low lateral etch rate due to the lower spontaneous reaction of Si with atomic bromine compared to that with chlorine. It is speculated that the slower resist erosion rate in bromine-containing plasma is attributable to the lower reactivity of Br atoms in attacking resist, compared to Cl atoms. Besides, the lower volatility of brominated erosion products may be another cause.[16] Also, they reported that since less resist erosion carbon-containig products are available, oxide etching is depressed.

In this paper, the composition and chemical bonds of poly-silicon etch residue were studied with XPS and SEM. From these results, the formation mechanism of etch residue were discussed.

Ⅱ. EXPERIMENTAL

Ⅱ-1. Sample Preparation

Samples used in this study were prepared as follows. 1000Å thermal oxide on a 6 inch bare wafer was grown in a O_2 stream furnace and then 5500Å polysilicon doped by $POCl_3$ was subsequently deposited by LPCVD (Low Pressure Chemical Vapor Deposition). The prepared samples were coated with positive PR (PhotoResist) and patterned by 64M DRAM S1 mask. The preparation process of the samples is shown schematically in Fig. 1.

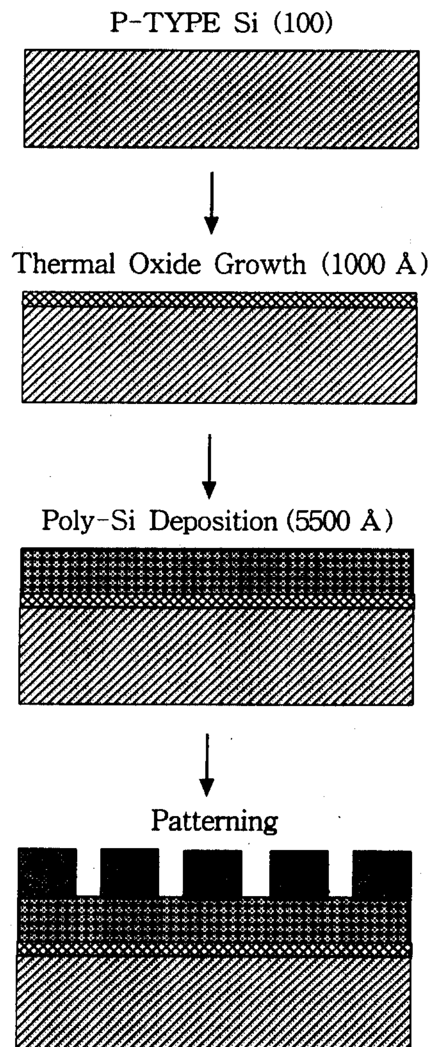

Fig. 1. A schematic diagram of the sample preparation procedure.

Ⅱ-2. Etching Apparatus and Principles

The samples were etched in a MERIE (Magnetically Enhanced Reactive Ion Etching) PRECISION 5000 etcher manufactured by Applied Material Inc. The structure of the polysilicon etch chamber was shown in Fig. 2. The backside of the chamber was cooled by He gas to keep a constant temperature and volatile etch products were pumped by the turbo pump. Since ion density generated in the plasma state is decreased due to low pressure chamber condition of the RIE (Reactive Ion Etching) etchers, the MERIE etchers with the magnets around the etch chamber have been developed to enhance ion density within the chamber, with the magnets around etch chamber, and etch rate by increasing ion residence time in plasma. The MERIE type etches materials by both chemical and physical phenomena simultaneously, that is, collisions between substrate and ions and reactions between the excited energetic atoms and substrate. The phenomena is due to the increased ion density by magnets attached around the chamber. Specially, magnets in the MERIE etcher control electronic geometry of generated ions and can reject ions from the wall using magnetic field.

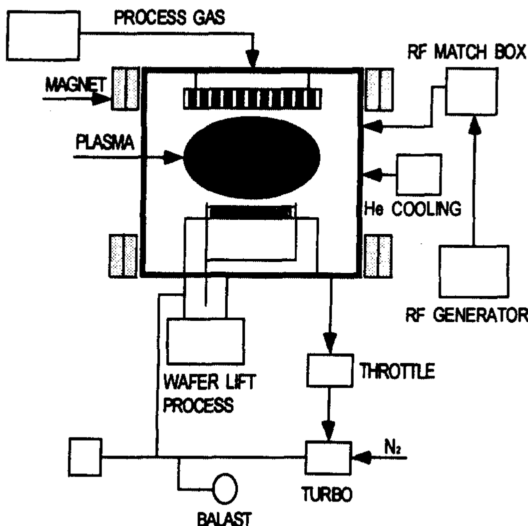

Fig. 2. A schematic diagram of MERIE etcher used in this experiment.

The MERIE etcher is effective in etching a material. Etch properties such as etch rate, selectivity are obtained predominant in the MERIE etcher rather than the RIE etcher. Plasma is generally generated by 13.56MHz RF power in the MERIE etcher.

Ⅱ-3. Experimental Procedure

The experimental procedure is shown simply in Fig. 1. A gas mixture of HBr, Cl_2 and He-O_2 was used for polysilicon etching. The experimental conditions were 150W RF power, 100mTorr pressure, 25℃ ground electrode temperature and 75Gauss magnetic field. The main steps in etching process were shown in Table 1. The breakthrough step was added in order to remove the native oxide due to air exposure of the sample, which can obstruct polysilicon etch. The etching end point was detected by monitoring CO peak during etch process and samples were overetched by 50 percent after EPD(End Point Detection) was detected.

Table 1. Polysilicon Etch Process Steps

	STEP 1 (Stabilization)	STEP 2 (Breakthrough)	STEP 3 (Stabilization)	STEP 4 (Main Etch)
Maximum Time	60 sec	15 sec	30 sec	600 sec
RF Power	0 W	200 W	0 W	150 W
Pressure	40mTorr	40mTorr	100mTorr	100mTorr
Max. Bias Field	-1000 V	-1000 V	-1000 V	-1000 V
Magnetic Field	0 Gauss	80 Gauss	75 Gauss	75 Gauss
Gases				
CF_4/O_2	30 sccm	30 sccm		
HBr			10 sccm	10 sccm
Cl_2			10 sccm	10 sccm
He-O_2			x sccm	x sccm

The effects of He-O_2 gas content, RF power and pressure on etch residue were investigated in this study. The He-O_2 content ratio was varied from 1 to 9, the RF power from 50W to 250W, and the pressure from 50mTorr

to 250mTorr. After samples were etched by the $HBr/Cl_2/He\text{-}O_2$ gas mixture, the photoresist was removed by Dry PR strip (using O_2 plasma) and WET PR strip (using O_3/H_2SO_4). Then, Surface layer chemistry has been characterized by XPS (X-ray Photoelectron Spectroscopy) or ESCA (Electron Spectroscopy of Chemical Analysis) [PERKIN-ELMER PHI 5400] and the morphology of the etched sample surface was investigated by SEM (Scannig Electron Microscopy) [Hitachi S5000].

Ⅲ. RESULTS

Ⅲ-1. Etch Characteristics of Polysilicon Etch Residue

Ⅲ-1-1. Chemistry dependence of polysilicon etch residue

Samples were etched in plasma state by the HBr, Cl_2 and $He\text{-}O_2$ gas mixtures. Fig. 3 shows the cross-section after just polysilicon etching. As shown in Fig. 3, photoresist mask was eroded during polysilicon etching. The erosion of photoresist mask for etching has been known to have a large effect on the residue formation. However, in addition to the effect of photoresist erosion, since $He\text{-}O_2$ content in the gas mixtures is considered to have a large effect on the polysilicon etch residue formation in this study, the polysilicon etch residue was investigated with the variation of $He\text{-}O_2$ content in the gas mixtures. Fig. 4 shows the effect of the $He\text{-}O_2$ content in the gas mixtures on the polysilicon etch residue after polysilicon etch and PR strip. Polysilicon etch residue was increased with increasing $He\text{-}O_2$ content. This is due to both increasing redeposition by collisions between etch products and increasing active species (ion, radical and atomic and molecular fragments) in plsama by oxygen addition. According to Ma et al.[16], the O_2 addition slightly enhanced the polysilicon etch rate, however the O_2 addition had to be controlled within 7% of total gas flow. Over the 7% of total gas, the excess O_2 shows the undesirable effects such as etch rate decrease, resist erosion and redeposition on the field. Fig. 5 shows the effect of the $He\text{-}O_2$ content on polysilicon etch rate. The polysilicon etch rate was monotonically increased with $He\text{-}O_2$ content, which is different from Ma et al.[16] This etch rate difference is caused by the fact that rede position at the PR sidewall is more dominant than at the etch pattern sidewall by the interaction between etch products and active species in plasma. In this study, $He\text{-}O_2$ gas was added to enhance polysilicon selectivity to PR. Increasing $He\text{-}O_2$ content also increase ion density in plasma state, which participates in

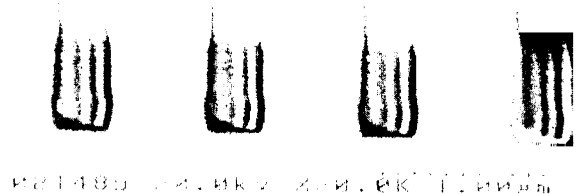

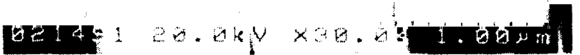

Fig. 3. SEM micrographs after just polysilicon etching at 150W RF power, 100mTorr pressure, and 30sccm HBr/ 30sccm Cl2/9 sccm $He\text{-}O_2$

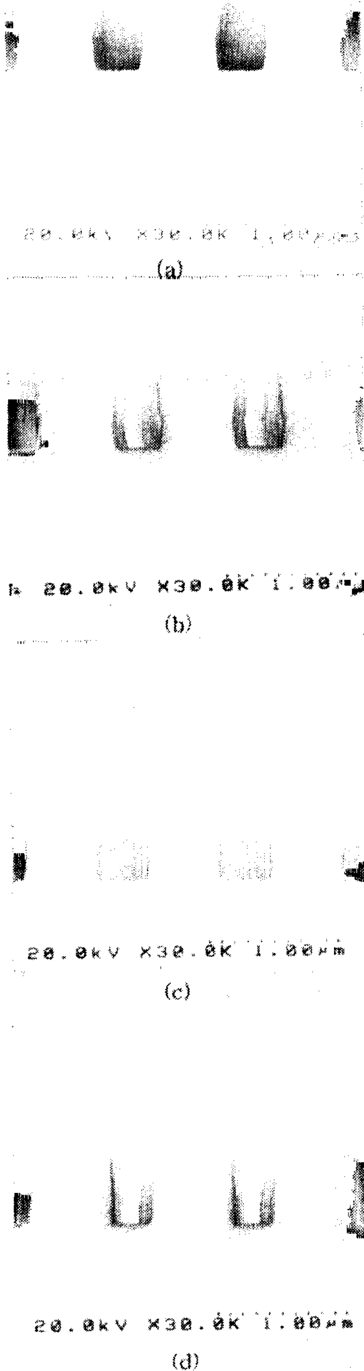

Fig. 4. SEM micrographs of polysilicon etch residue with He-O2 content of gas mixture after PR strip. The Experimenatal conditions are 150W RF power, 100mTorr pressure and HBr : Cl 2 : He-O2=10 : 10 : x
(a) x=1 (b) x=2 (3) x=3 (4) x=4

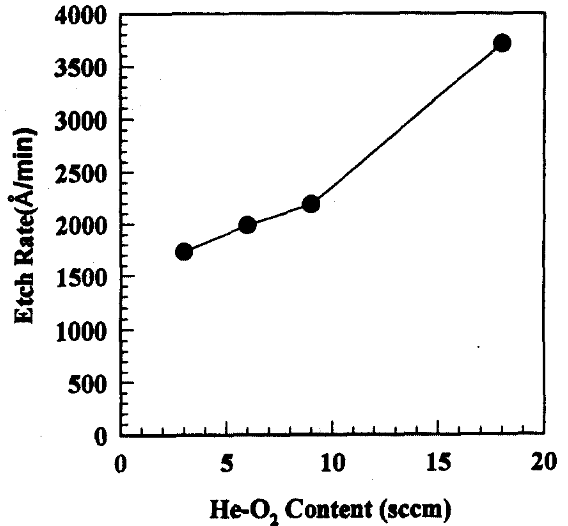

Fig. 5. Polysilicon etch rate as a function of He-O_2 content in HBr/Cl2/He-O_2 at 150W RF power and 10mTorr pressure.

polysilicon etching, and these active species increase polysilicon etch rate. However, the formed polysilicon etch residue is considered as a non-protector of polysilicon sidewall because of redeposition of PR sidewall when polysilicon is etched. As a result, polysilicon etch rate is mainly increased by active species in plasma state.

Ⅲ-1-2. RF power dependence on the polysilicon etch residue

The effect of RF power on the polysilicon etch residue was investigated for various RF powers. The experiment was performed by the power variation between 50W and 250W. The results are shown in Fig. 6. The polysilicon etch residue formations was independent on the RF power variation. According to Oehrlein et al.[18], fluorocarbon deposition rate was monotonically increased with increasing RF power, when silicon dioxide etched by CHF_3 and CF_4, respectively. Generally, increasing RF power enhances ion density of plasma state within an etch chamber. Deposition rate of polysilicon etch residue at the etched polysilicon sidewall is considered to be high at low RF power. High deposition rate is due to neutrals in plasma and as shown in Fig. 6

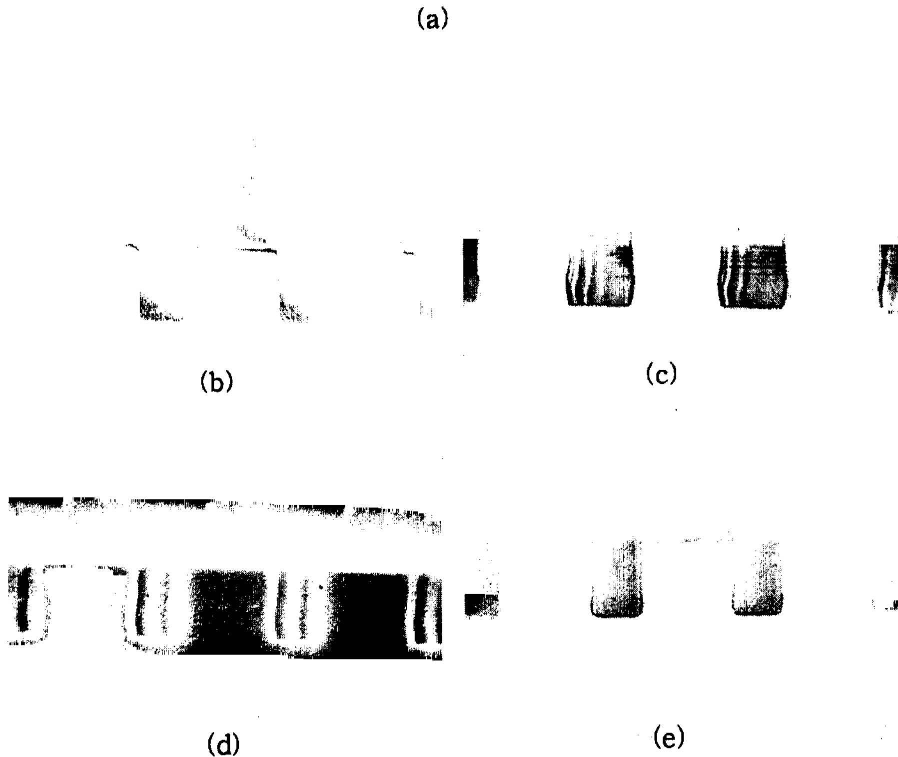

Fig. 6. SEM micrographa of RF power dependence of polysilicon etch residue at various RF powers, 100mTorr pressure, and 30 sccm HBr/30sccm Cl_2/9sccm He-O_2.
(a) 50 W (b) 100 W (c) 150 W (d) 200 W (e) 250 W

(a), polysilicon etch residue deposition results in the characteristic V-shape sloped profile. As RF power increases, deposition rate of poly-silicon etch residue was relatively decreased since polysilicon etch rate and volatility of the products were increased with RF power. As a result, low deposition rate caused anisotrpic etch profile as shown in Fig. 6 (e). In Fig. 7 polysilicon etch rates are shown as a function of RF power. Increasing RF power enhances polysilicon etch rate and the result was consistent with many researchers[12),13),16)]. It is considered that the ion etching increased by ion density enhancement results.

Ⅲ-1-3. Pressure dependence of polysilicon etch residue

Pressure is also an important variable having an effect on etching characteristics. For example, variation of pressure affects etch

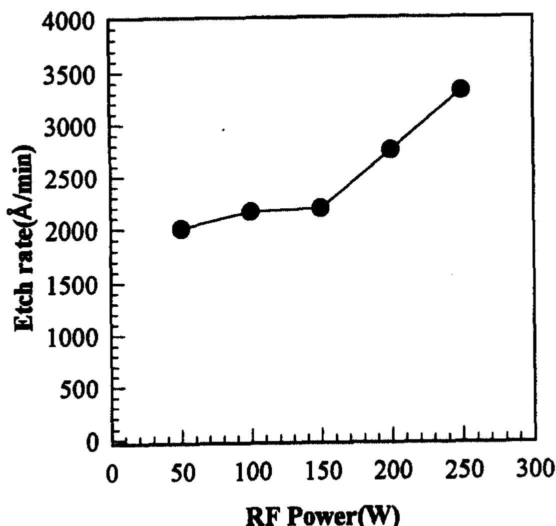

Fig. 7. Polysilicon etch rate as a function of RF power at 100 mTorr pressure and 30 sccm HBr/ 30 sccm Cl_2/ 9sccm He-O_2

rate, selectivity, uniformity and so on. Fig. 8 shows the pressure dependence of polysilicon etch residue formation. The polysilicon etch residue formation was independent on the pressure variation. Most of the polysilicon etch residue existed on the top of etched polysilicon surface regardless of the pressure variation. As shown in Fig. 8 (a), the polysilicon sidewall deposition rate of etch residue is considered to be low at low pressure compared with the polysilicon etch rate. This result is the same as that for the high RF power. Also, as pressure is increased, the deposition rate of polysilicon etch residue at polysilicon sidewall increased. It is partially due to suppression of volatile etch products in high pressure. The polysilicon etch rate was shown as a function of pressure in Fig. 9. The maximum etch rate within the applied extend was shown at 150mTorr pressure.

Ⅲ-2. Polysilicon Etch Residue Analysis by XPS

As mentioned previously, XPS is a predominant surface analysis equipment to analyze bond forms and constituent elements of materials such as thin solid films, gas state and liquid state.[21] The polysilicon etch residue was characterized by XPS. Fig. 10 shows wide scan data of XPS after PR strip. Most of the constituent elements of the polysilicon etch residue were silicon and oxygen. A carbon element peak was also detected, however it is considered as an unimportant component, since this carbon component is thought to be caused by air exposure before XPS analysis. High resolution spectrum for the main components, that is, Si, O, C, was taken to analyze chemical bond form and existing zone. Fig. 11 shows Si_{2p}, O_{1s} and C_{1s} narrow scan data in case of 9sccm He-O_2 . The XPS spectra show three binding forms in Si_{2p} peak, two binding forms in O_{1s} peak and one binding form in C_{1s} peak. Their binding energies are listed in Table 2.

Table 2. Binding Energies of XPS Spectrum at 75° Take-off Angle after Polysilicon Etching

volumetric ratio of gas mixture		Chemical bond forms	Binding energy(eV)
10 : 10 : 1	Si_{2p}	Si-Si	100.5
		Si-O (thermal)	104.4
		Si-O (residue)	104.7
	O_{1s}	Si-O (thermal)	532.7
		Si-O (residue)	532.9
	C_{1s}	C-C or C-H	286.2
10 : 10 : 3	Si_{2p}	Si-Si	100.2
		Si-O (thermal)	104.4
		Si-O (residue)	106.2
	O_{1s}	Si-O (thermal)	533.7
		Si-O (residue)	535.6
	C_{1s}	C-C or C-H	287.5

In case of larger He-O_2 content, The XPS analysis data show more clear intensity difference among residue peak and the other peaks. It indirectly demonstrates polysilicon etch residue is increased with increasing He-

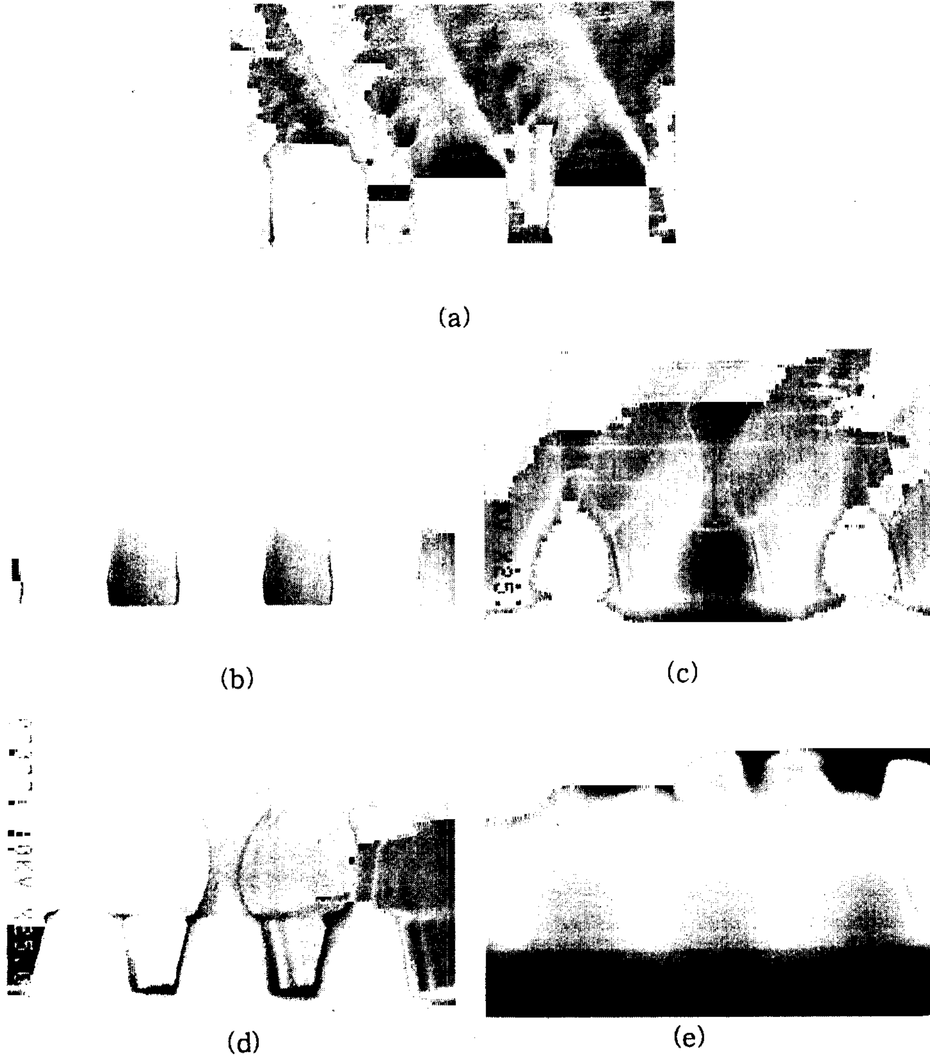

Fig. 8. SEM micrographs of pressure dependence of polysilicon etch residue at various pressure, 150W RF power and 30 sccm HBr/30sccm Cl_2/9sccm He-O_2.
(a) 50 mTorr (b) 100 mTorr (c) 150 mTorr (d) 200 mTorr (e) 250 mTorr

O_2 content. As shown in Table 2, the binding energies of polysilicon etch residue with He-O_2 ratio showed 104.7eV and 106.2eV for Si_{2p} spectrum and 532.9eV and 535.6eV for O_{1s} spectrum, respectively. Since main constituent compositions of the polysilicon etch residue are silicon and oxygen and binding energy of the residue is larger than thermal oxide (SiO_2), the most stable silicon oxide having the most largest binding energy, a chemical bonding form of the polysilicon etch residue has been considered as SiO_x ($x>2$). The etched surface also is analyzed by take-off angle variations (15°, 45° and 75°) to enhance sensitivity. When polysilicon etch residue peak is compared to other peaks, the intensity of polysilicon etch residue is larger than others in take-off angle of 15°. This demonstrates that most of the polysilicon etch residue exists on the top of the etched polysilicon pattern in accordance with the results of Fig. 3.

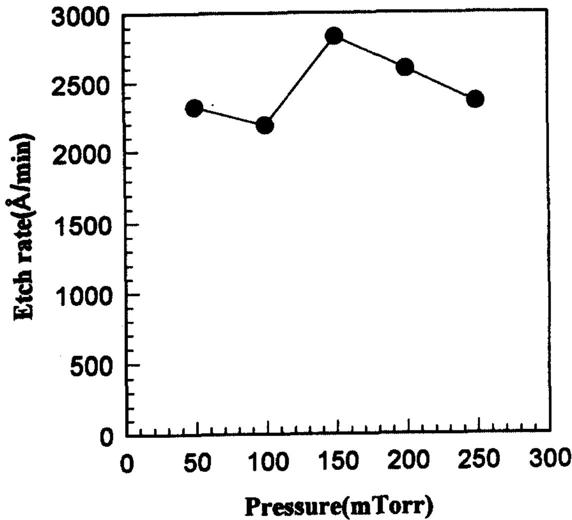

Fig. 9. Polysilicon etch rate as a function of pressure at 150 W RF power and 30 sccm HBr/ 30sccm Cl_2/ 9sccm He- O_2.

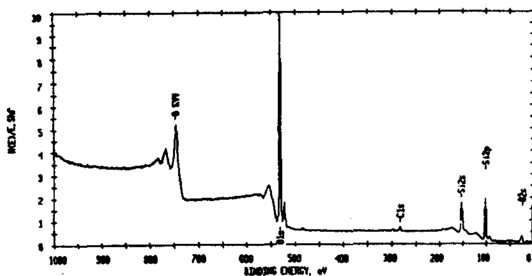

Fig. 10. The XPS survey spectrum after polysilicon etching at 150 W RF power, 100mTorr pressure and 30sccm HBr/ 0sccm Cl_2/9sccm He-O_2 and PR strip.

The depth profile of the sample is also taken successively by Ar sputtering during 10 minutes as shown in Fig. 12. As the sample was sputtered by Ar atoms or Ar^+ ions, the polysilicon etch residue was removed from the sample surface with sputtering time and the polysilicon intensity was increased gradually by the exposure of polysilicon sublayer. After 10 minutes Ar sputtering, the polysilicon etch residue was completely removed from the sample surface and only polysilicon and thermal oxide peaks were detected in the depth profile spectrum. As a result, the depth profile shows that the etched surface consists of an oxide-like residue layer and a thermal oxide or polysilicon layer after etching.

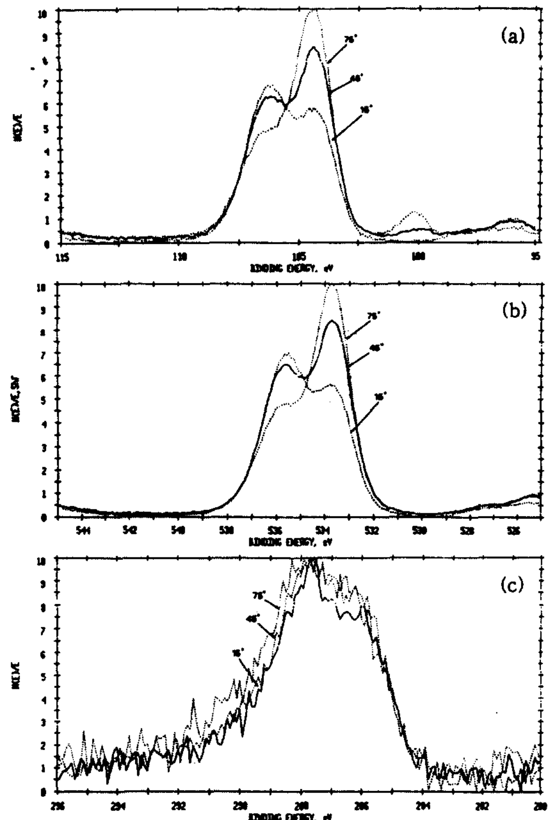

Fig. 11. The high resolution XPS spectra of the sample etched at 150W RF power, 100mTorr pressure and 30 sccm HBr/ 30sccm Cl_2/ 9sccm He-O_2
(a) Si_{2p} spectrum (b) O_{1s} spectrum
(c) C_{1s} spectrum

Ⅳ. CONCLUSIONS

The polysilicon etch residue characteristics were studied as a function of He-O_2 content, RF power and pressure in this study. The polysilicon etch residue formed during etching by HBr/Cl_2/He-O_2 mixture was increased with increasing He-O_2 content. Most of the polysilicon etch residue was formed onto the top of etched polysilicon pattern. The polysilicon etch

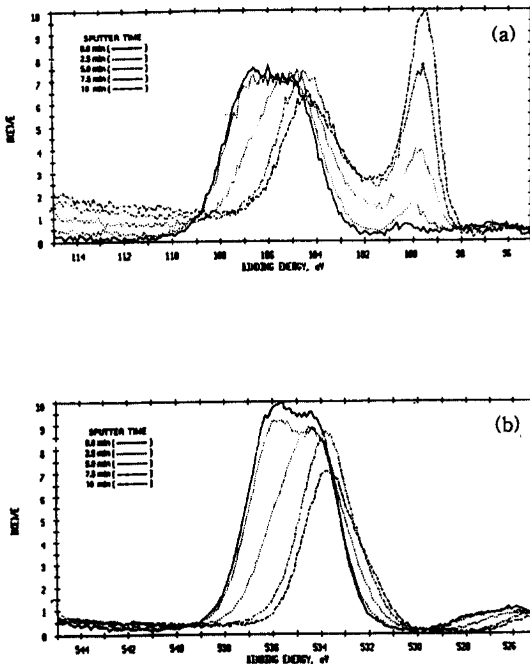

Fig. 12. The depth profile of the sample etched at 150W RF power, 100mTorr pressure and 30 sccm HBr/ 30sccm Cl_2/ 9sccm He-O_2.
(a) Si_{2p} spectrum (b) O_{1s} spectrum

rate was monotonically increased with He-O_2 content. The polysilicon etch residue was not affected by RF power and pressure variation. The deposition rate of the polysilicon etch residue onto the polysilicon sidewall was high at low RF power and high pressure. As a result, the polysilicon etch residue deposition resulted in the characteristic V-shape sloped profile. The polysilicon etch residue was characterized by the XPS. The binding energy of the polysilicon etch residue was larger than that of thermal oxide which was considered as the most stable silicon oxide. Therefore, the formed etch residue was considered as an oxide-like residue having $SiO_x(x>2)$ chemical bond.

ACKNOWLEDGEMENT

The authers wish to acknowledge the financial support of the Korea Research Foundation made in Program Year 1996.

REFERENCES

1. Coburn, J. W. and Eric Kay, Solid State Technology, 117(1979).
2. Yih, P. H. and Steckl, A. J., J. Electrochem. *Soc.*, **140(6)**, 1813(1993).
3. Simko, J. P. and Oehrlein, G. S., J. Electrochem. Soc., **138(9)**, 2748(1991).
4. Oehrlein, G. S., Tromp, R. M., Tsang, J. C., Lee, Y. H. and Petrillo, E. J., J. Electrochem. Soc., **132(6)**, 1441(1985).
5. Coyle, Jr., G. J. and Oehrlein, G. S., Appl. Phys. Lett., **47(6)**, 604(1985).
6. Oehrlein, G. S., Clabes, J. G. and Spirito, P., J. Electrochem. Soc., **133(5)**, 1002 (1986).
7. Potter, G. E. and Morrison, G. H. , J. Vac. Sci. Technol. **B10(6)**, 2398(1992).
8. Oehrlein, G. S. and Williams, H. L., J. Appl. Phys. **62(2)**, 662(1987).
9. Oehrlein, G. S., Robey, S. W. and Lindström, J. L. , Appl. Phys. Lett., **52(14)**, 1170(1988).
10. Barklund, A. M. and Blom, H. -O. , J. Vac. Sci. Technol., **A10(4)**, 1212(1992).
11. Meyyappan, M., McLane, G. F., Cole, M. W., Laraeu, R., Namaroff, M., Sasserath, J. and Sundararaman, C. S. , J. Vac. Sci. Technol., **A10(4)**, 1147(1992).
12. Oehrlein, G. S., Zhang, Y., Vender, D. and Haverlag, M. , J. Vac. Sci. Technol., **A12(2)**, 323(1994).
13. Oehrlein, G. S., Zhang, Y., Vender, D. and Joubert, O., J. Vac. Sci. Technol., **A12(2)**, 333(1994).
14. Gray, D. C., Mohindra, V. and Sawin, H. H., J. Vac. Sci. Technol., **A12(2)**, 354(1994)
15. Yeom, G. Y., Ono, Y. and Yamaguchi, T. , J. Electrochem. Soc., **139(2)**, 575(1992).
16. Ma, D. X., Lin, T. A. and Chen, C. H. , J. Vac. Sci. Technol., **A10(4)**, 1217(1992).
17. Pearton, S. J., Chakrabarti, U. K., Lone, E., Perley, A. P., Abernathy, C. R., Hobson, W. S. and Jones, K. S., J. Electrochem. Soc.,

17. Pearton, S. J., Chakrabarti, U. K., Lone, E., Perley, A. P., Abernathy, C. R., Hobson, W. S. and Jones, K. S., J. Electrochem. Soc., **139(3)**, 856(1992).
18. Fujino, K. and Oku, T., J. Electrochem. Soc., **139(9)**, 2585(1992).
19. Sparks, D. R., J. Electrochem. Soc., **139(6)**, 1736(1992).
20. Tsou, L. Y., *J.* Electrochem. Soc., **136(10)**, 3003(1989).
21. Grasserbauer, M. and Werner, H. W., "Analysis of Microelectronic Materials and Devices" (1991)